arXiv:hep-lat/0310018v1 7 Oct 2003

A NEW METHOD FOR SIMULATING QCD AT FINITE DENSITY

JUN NISHIMURA

High Energy Accelerator Research Organization (KEK),
1-1 Oho, Tsukuba 305-0801, Japan
E-mail: jnishi@post.kek.jp

We propose a new method for simulating QCD at finite density, where interesting phases such as the color superconductivity phase is conjectured to appear. The method is based on a general factorization property of distribution functions of observables, and it is therefore applicable to any system with a complex action. The so-called overlap problem is completely eliminated by the use of constrained simulations. We test this method in a Random Matrix Theory for finite density QCD, where we are able to reproduce the exact results for the quark number density. The achieved system size is large enough to extract the thermodynamic limit. Our results provide a clear understanding of how the expected first order phase transition is induced by the imaginary part of the action. We also discuss the non-commutativity of the zero chemical potential limit ($\mu \to 0$) and the thermodynamic limit, which is relevant to recent Monte Carlo studies at small μ.

1. Introduction

Recently there are a lot of activities in QCD at finite density, where interesting phases such as a superconducting phase have been conjectured to appear [1]. At zero chemical potential Monte Carlo simulations of lattice QCD enable nonperturbative studies from first principles. It is clearly desirable to extend such an approach to finite density and explore the phase diagram of QCD in the T(temperature)-μ(chemical potential) plane. The main obstacle here is that the Euclidean action becomes complex once the chemical potential is switched on.

Nevertheless QCD at finite density has been studied by various approaches with exciting conjectures. First there are perturbative studies which are valid in the $\mu \to \infty$ limit [2,3]. Refs. [4] and [5] use effective theories with instanton-induced four-fermi interactions. As for Monte Carlo studies two directions have been pursued so far. One is to modify the model so that the action becomes real. This includes changing the gauge group

from SU(3) to SU(2) [6], and introducing a chemical potential with opposite signs for up and down quarks [7]. The other direction is to explore the large T and small μ regime of lattice QCD, where the imaginary part of the action is not very large [8,9,10,11]. These studies already produced results relevant to heavy ion collision experiments, but more interesting physics will be uncovered if larger μ regime becomes accessible by simulations.

In Ref. [12] we have proposed a new method to simulate systems with a complex action, which utilizes a simple factorization property of distribution functions of observables. Since the property holds quite generally, the approach can be applied to any system with a complex action. The most important virtue of the method is that it eliminates the so-called overlap problem, which occurs in the standard re-weighting method. Ultimately we hope that this method will enable us, among other things, to explore the phase diagram of QCD at finite baryon density.

As a first step we test [13] the new approach in a Random Matrix Theory, which can be regarded as a schematic model for QCD at finite baryon density [14]. We also present preliminary results [15], which reveal certain noncommutativity of the $\mu \to 0$ limit and the thermodynamic limit.

2. Brute-force approach —reweighting method—

Suppose we want to study the model defined by the partition function

$$Z = \int \mathrm{d}U \, \mathrm{e}^{-S_0 + i\,\Gamma} \ , \tag{2.1}$$

where S_0 and Γ are real. Since the weight $\mathrm{e}^{-S_0+i\,\Gamma}$ in (2.1) is not positive definite, we cannot regard it as a probability density. Hence it seems difficult to apply the idea of standard Monte Carlo simulations, which reduces the problem of obtaining vacuum expectation values (VEVs) to that of taking an average over an ensemble generated by the probability. One way to proceed is to apply the reweighting method and rewrite the VEV $\langle \mathcal{O} \rangle$ as

$$\langle \mathcal{O} \rangle = \frac{\left\langle \mathcal{O}\, \mathrm{e}^{i\Gamma} \right\rangle_0}{\left\langle \mathrm{e}^{i\Gamma} \right\rangle_0} \ , \tag{2.2}$$

where the symbol $\langle \, \cdot \, \rangle_0$ denotes a VEV with respect to the *phase-quenched* partition function

$$Z_0 = \int \mathrm{d}U \, \mathrm{e}^{-S_0} \ . \tag{2.3}$$

Since the system (2.3) has a positive definite weight, the VEV $\langle \, \cdot \, \rangle_0$ can be evaluated by standard Monte Carlo simulations. However, the fluctuations

of the phase Γ in (2.2) grows linearly with the system size V. Due to huge cancellations, both the denominator and the numerator of the r.h.s. of (2.2) vanish as $\mathrm{e}^{-\mathrm{const.}V}$ as V increases, while the 'observables' $\mathrm{e}^{i\Gamma}$ and $\mathcal{O}\mathrm{e}^{i\Gamma}$ are of O(1) for each configuration. As a result, the number of configurations required to obtain the VEVs with some fixed accuracy grows as $\mathrm{e}^{\mathrm{const.}V}$. This is the notorious 'complex-action problem'. Moreover when one simulates the phase-quenched model (2.3), one cannot sample efficiently the configurations which are relevant to the calculation of the VEV $\langle\mathcal{O}\rangle$. This is the so-called 'overlap problem'.

3. New approach — factorization method —

In the factorization method proposed in Ref. [12], the fundamental objects are the distribution functions (we assume the observable $\mathcal{O}$ to be real)

$$\rho(x) \stackrel{\mathrm{def}}{=} \langle\delta(x-\mathcal{O})\rangle \tag{3.1}$$

$$\rho^{(0)}(x) \stackrel{\mathrm{def}}{=} \langle\delta(x-\mathcal{O})\rangle_0 \tag{3.2}$$

defined for the full model (2.1) and for the phase-quenched model (2.3), respectively. The important property of $\rho(x)$ is that it factorizes as

$$\rho(x) = \frac{1}{C}\,\rho^{(0)}(x)\,\varphi(x)\ , \tag{3.3}$$

where the constant C is given by $C \stackrel{\mathrm{def}}{=} \langle\mathrm{e}^{i\,\Gamma}\rangle_0$. The 'weight factor' $\varphi(x)$, which represents the effect of Γ, can be written as a VEV

$$\varphi(x) \stackrel{\mathrm{def}}{=} \langle\mathrm{e}^{i\,\Gamma}\rangle_x \tag{3.4}$$

with respect to yet another partition function

$$Z(x) = \int \mathrm{d}U\,\mathrm{e}^{-S_0}\,\delta(x-\mathcal{O})\ . \tag{3.5}$$

The δ-function represents a constraint on the system. In actual simulation we replace the δ-function by a sharply peaked potential. The distribution $\rho^{(0)}(x)$ for the phase-quenched model can also be obtained from the same simulation. Then the VEV $\langle\mathcal{O}\rangle$ can be obtained by

$$\langle\mathcal{O}\rangle = \int \mathrm{d}x\,x\,\rho(x) = \frac{\int \mathrm{d}x\,x\,\rho^{(0)}(x)\,\varphi(x)}{\int \mathrm{d}x\,\rho^{(0)}(x)\,\varphi(x)}\ , \tag{3.6}$$

where the overlap problem is eliminated by forcing the simulation to sample the important configurations by the constraint. The knowledge of the weight factor $\varphi(x)$ is useful because it tells us precisely which values of $\mathcal{O}$

are favored or disfavored by the effects of the oscillating phase. Once a rough estimate of $\rho(x)$ is obtained, one may perform multi-canonical simulations with an appropriate weight (instead of simulating (3.5) for many x) to sample relevant configurations more efficiently. This has not yet been done, however.

4. Random Matrix Theory for finite density QCD

The Random Matrix Theory we study is defined by the partition function

$$Z = \int \mathrm{d}W \mathrm{e}^{-N \,\mathrm{tr}(W^\dagger W)} \,\det D \;, \tag{4.1}$$

where W is a $N \times N$ complex matrix, and D is a $2N \times 2N$ matrix given by

$$D = \begin{pmatrix} m & iW + \mu \\ iW^\dagger + \mu & m \end{pmatrix} \;. \tag{4.2}$$

The parameters m and μ correspond to the 'quark mass' and the 'chemical potential', respectively. The fermion determinant becomes complex for $\mu \neq 0$, so we write it as $\det D = \mathrm{e}^{i\Gamma} \,|\det D|$. The complex-action problem arises due to the phase Γ. In what follows we consider the massless case ($m = 0$) for simplicity and focus on the 'quark number density' defined by

$$\nu = \frac{1}{2N} \,\mathrm{tr}\, \left(\gamma_4 D^{-1}\right) \;, \qquad \gamma_4 = \begin{pmatrix} 0 & \mathbb{1} \\ \mathbb{1} & 0 \end{pmatrix} \;. \tag{4.3}$$

The model was first solved in the large-N limit [14], and turned out to be solvable later even for finite N [16]. The partition function can be expressed as

$$Z(\mu, N) = \pi \mathrm{e}^{\kappa} N^{-(N+1)} \, N! \left[1 + \frac{(-1)^{N+1}}{N!} \gamma(N+1, \kappa)\right] \;, \tag{4.4}$$

where $\kappa = -N\mu^2$ and $\gamma(n, x)$ is the incomplete γ-function defined by

$$\gamma(n, x) = \int_0^x \mathrm{e}^{-t} \, t^{n-1} \, \mathrm{d}t \;. \tag{4.5}$$

From this one obtains the VEV of the quark number density as

$$\langle \nu \rangle = \frac{1}{2N} \frac{\partial}{\partial \mu} \ln Z(\mu, N) \tag{4.6}$$

$$= -\mu \left[1 + \frac{\kappa^N \mathrm{e}^{-\kappa}}{(-1)^{N+1} N + \gamma(N+1, \kappa)}\right] \;. \tag{4.7}$$

Taking the large-N limit, one obtains

$$\lim_{N\to\infty}\langle\nu\rangle = \begin{cases} -\mu & \text{for } \mu < \mu_{\rm c} \\ 1/\mu & \text{for } \mu > \mu_{\rm c}\ , \end{cases} \tag{4.8}$$

where $\mu_{\rm c}$ is the solution to the equation $1+\mu^2+\ln(\mu^2)=0$, and its numerical value is given by $\mu_{\rm c} = 0.527\cdots$. We find that the quark number density $\langle\nu\rangle$ has a discontinuity at $\mu=\mu_{\rm c}$. Thus the schematic model reproduces qualitatively the first order phase transition expected to occur in 'real' QCD at nonzero baryon density.

The phase-quenched model defined by the partition function

$$Z_0 = \int {\rm d}W {\rm e}^{-N\,{\rm tr}(W^\dagger W)}\,|\det D| \tag{4.9}$$

can be solved in the large N limit [14] and one obtains

$$\lim_{N\to\infty}\langle\nu\rangle_0 = \begin{cases} \mu & \text{for } \mu < 1 \\ 1/\mu & \text{for } \mu > 1\ , \end{cases} \tag{4.10}$$

which is a continuous function of the chemical potential μ unlike (4.8). Thus the first order phase transition in the full model (4.1) occurs precisely due to the imaginary part Γ of the action. This model therefore provides a nice testing ground for simulation techniques for finite density QCD [14].

5. Testing the factorization method in the RMT

Since ν is complex for each configuration, we decompose it into the real and imaginary parts as $\nu=\nu_{\rm R}+i\nu_{\rm I}$ and calculate $\langle\nu_{\rm R}\rangle$ and $\langle\nu_{\rm I}\rangle$ by the factorization method ($\langle\nu_{\rm I}\rangle$ is purely imaginary). We introduce the distribution functions for $\nu_{\rm R}$ and $\nu_{\rm I}$ separately as

$$\rho_i(x) \stackrel{\rm def}{=} \langle\delta(x-\nu_i)\rangle \qquad i={\rm R,I}\ , \tag{5.1}$$

$$\rho_i^{(0)}(x) \stackrel{\rm def}{=} \langle\delta(x-\nu_i)\rangle_0 \qquad i={\rm R,I}\ . \tag{5.2}$$

The factorization holds for both $\rho_{\rm R}(x)$ and $\rho_{\rm I}(x)$ as

$$\rho_i(x) = \frac{1}{C}\,\rho_i^{(0)}(x)\,\varphi_i(x) \qquad i={\rm R,\ I}\ , \tag{5.3}$$

where the constant C is given by $C \stackrel{\rm def}{=} \langle {\rm e}^{i\,\Gamma}\rangle_0$. The weight factors $\varphi_i(x)$ can be written as a VEV

$$\varphi_i(x) \stackrel{\rm def}{=} \langle {\rm e}^{i\,\Gamma}\rangle_{i,\,x} \qquad i={\rm R,\ I} \tag{5.4}$$

with respect to the constrained phase-quenched model

$$Z_i(x) = \int \mathrm{d}W \, \mathrm{e}^{-N \,\mathrm{tr}(W^\dagger W)} \, |\det D| \, \delta(x - \nu_i) \qquad i = \mathrm{R},\, \mathrm{I} \; . \tag{5.5}$$

Under the transformation $W \mapsto -W$, the Gaussian action is invariant, whereas the fermion determinant $\det D$ as well as the quark number density ν becomes complex conjugate. Due to this symmetry, we have

$$\varphi_{\mathrm{R}}(x)^* = \varphi_{\mathrm{R}}(x) \; , \tag{5.6}$$

$$\varphi_{\mathrm{I}}(x)^* = \varphi_{\mathrm{I}}(-x) \; , \tag{5.7}$$

$$\rho_{\mathrm{I}}^{(0)}(-x) = \rho_{\mathrm{I}}^{(0)}(x) \; . \tag{5.8}$$

Using these properties, we arrive at

$$\langle \nu_{\mathrm{R}} \rangle = \frac{1}{C} \int_{-\infty}^{\infty} \mathrm{d}x \, x \, \rho_{\mathrm{R}}^{(0)}(x) \, w_{\mathrm{R}}(x) \; , \tag{5.9}$$

$$\langle \nu_{\mathrm{I}} \rangle = \frac{2\,i}{C} \int_{0}^{\infty} \mathrm{d}x \, x \, \rho_{\mathrm{I}}^{(0)}(x) \, w_{\mathrm{I}}(x) \; , \tag{5.10}$$

$$C = \int_{-\infty}^{\infty} \mathrm{d}x \, \rho_{\mathrm{R}}^{(0)}(x) \, w_{\mathrm{R}}(x) \; , \tag{5.11}$$

where the weight factors $w_i(x)$ are defined by

$$w_{\mathrm{R}}(x) \stackrel{\mathrm{def}}{=} \langle \cos \Gamma \rangle_{\mathrm{R},x} \tag{5.12}$$

$$w_{\mathrm{I}}(x) \stackrel{\mathrm{def}}{=} \langle \sin \Gamma \rangle_{\mathrm{I},x} = -w_{\mathrm{I}}(-x) \; . \tag{5.13}$$

Table 1. Results of the analysis of $\langle \nu \rangle$ described in the text. Statistical errors computed by the jackknife method are shown. The last column represents the exact result for $\langle \nu \rangle$ at each μ and N. For $\mu = 0.2$ the exact result is $\langle \nu \rangle = -0.2$ with an accuracy better than 1 part in 10^{-9}.

μ	N	$\langle \nu_{\mathrm{R}} \rangle$	$i \langle \nu_{\mathrm{I}} \rangle$	$\langle \nu \rangle$	$\langle \nu \rangle$ (exact)
0.2	8	0.0056(6)	-0.1970(5)	-0.1915(7)	-0.20000...
0.2	16	0.0060(4)	-0.1905(13)	-0.1845(13)	-0.20000...
0.2	24	0.0076(9)	-0.1972(14)	-0.1896(17)	-0.20000...
0.2	32	0.0021(8)	-0.1947(19)	-0.1927(25)	-0.20000...
0.2	48	0.0086(37)	-0.2086(54)	-0.2000(88)	-0.20000...
1.0	8	0.8617(10)	0.1981(13)	1.0598(12)	1.066501...
1.0	16	0.8936(2)	0.1353(6)	1.0289(5)	1.032240...
1.0	32	0.9207(1)	0.0945(2)	1.0152(3)	1.015871...

In Table 1 we show our results for two values of μ, $\mu = 0.2$ and $\mu = 1.0$, which are on opposite sides of the first order phase transition point $\mu =$

$\mu_{\rm c} = 0.527\cdots$. They are in good agreement with the exact results, and the achieved values of N are large enough to extract the large N limit.

In Fig. 1 we plot $w_{\rm R}(x)$ for $N = 8$ at various μ. It is interesting that the $w_{\rm R}(x)$ changes from positive to negative for $\mu < \mu_{\rm c}$, but it changes from negative to positive for $\mu > \mu_{\rm c}$. (Similarly $w_{\rm I}(x)$ is positive at $x > 0$ for $\mu < \mu_{\rm c}$, but it is negative at $x > 0$ for $\mu > \mu_{\rm c}$.) Thus the behavior of $w_i(x)$ changes drastically as the chemical potential μ crosses its critical value $\mu_{\rm c}$. These results provide a clear understanding of how the first order phase transition occurs due to the effects of Γ. Fig. 2 shows the results for $\langle\nu\rangle$ obtained by the factorization method for $N = 8$ at various μ, which nicely reproduce the gap developing at the critical point.

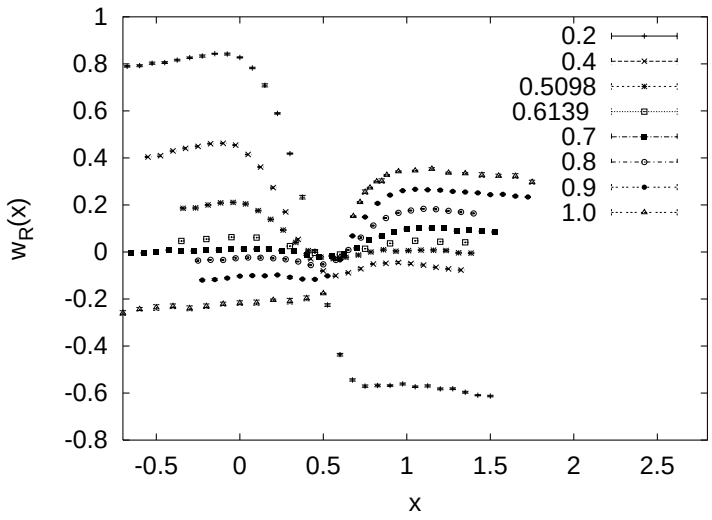

Figure 1. The weight factor $w_{\rm R}(x)$ is plotted for $N = 8$ at various μ.

6. Noncommutativity of $\mu \to 0$ and $N \to \infty$

In this Section we discuss the noncommutativity of the two limits, $\mu \to 0$ and $N \to \infty$. The absence of such noncommutativity is implicitly assumed in most of the recent approaches used in simulating finite density QCD at small μ. This includes the multi-parameter reweighting approach [8], the Taylor expansion approach [9], and the imaginary μ approach [10,11]. In all

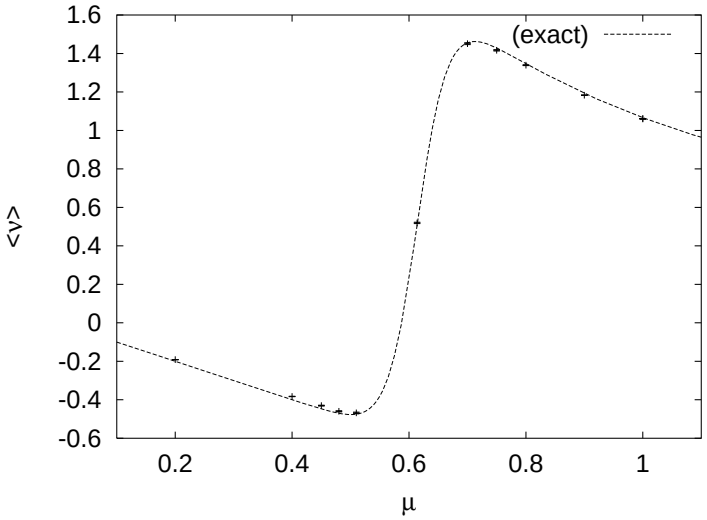

Figure 2. The VEV $\langle\nu\rangle$ obtained by the factorization method is plotted against μ for $N = 8$ including the critical regime. Statistical errors computed by the jackknife method are also shown. The dashed line represents the exact result (4.7) for $\langle\nu\rangle$ at $N = 8$.

these works one restricts oneself to the small μ regime where the fluctuation of the phase is still under control.

In fact the noncommutativity can be readily seen from the exact result (4.4) for the partition function (4.1). The phase of the determinant vanishes at $\mu = 0$ for finite N, and one obtains a nonzero result for the partition function $Z = 1$ in the large N limit. On the other hand, the oscillation of the phase becomes pronounced at sufficiently large N even for small but finite μ, and as a result one obtains $Z = 0$ in the large N limit as far as μ is kept finite. This implies in particular that the free energy

$$f(\mu) = -\lim_{N\to\infty} \frac{1}{N^2} \ln Z(\mu, N) \tag{6.1}$$

has a discontinuity at $\mu = 0$ as

$$\lim_{\mu\to 0} f(\mu) > f(0) = 0 \ . \tag{6.2}$$

We expect that, in general, the free energy of a system with a complex action has a discontinuity at a point in the parameter space where the imaginary part of the action vanishes identically.

With the factorization method we can take the two limits $\mu \to 0$, $N \to \infty$ in different orders and compare the results. As we will see, we

do observe the noncommutativity in various ways. On the other hand, we know from the exact result (4.7) that the VEV $\langle\nu\rangle$ does not have the noncommutativity. In the factorization method $\langle\nu\rangle = \langle\nu_{\rm R}\rangle + i\langle\nu_{\rm I}\rangle$ is calculated by the formulae (5.9), (5.10) and (5.11). In fact the functions $w_{\rm R}(x)$, $w_{\rm I}(x)$ and $\rho_{\rm R}^{(0)}(x)$ have the noncommutativity, but these effects cancel each other in the end results for $\langle\nu_{\rm R}\rangle$ and $\langle\nu_{\rm I}\rangle$. In what follows we present preliminary results relevant to $\langle\nu_{\rm R}\rangle$, but similar results are obtained for $\langle\nu_{\rm I}\rangle$ as well [15].

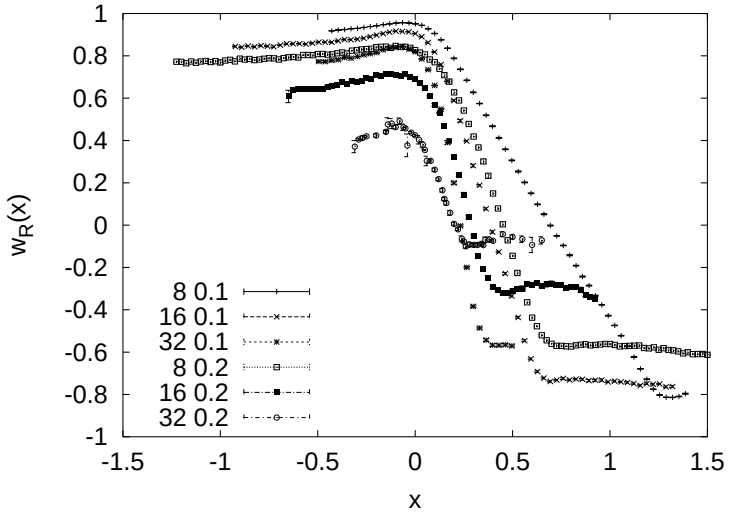

Figure 3. The weight factor $w_{\rm R}(x)$ is plotted for $\mu = 0.1$ and 0.2 at $N = 8, 16, 32$.

Let us first look at the weight factor $w_{\rm R}(x)$, which has the noncommutativity similar to the partition function. At $\mu = 0$ one obtains $w_{\rm R}(x) \equiv 1$ for any N, whereas in the large N limit one obtains $w_{\rm R}(x) \equiv 0$ for any μ. In Fig. 3 we plot $w_{\rm R}(x)$ for $\mu = 0.1$ and $\mu = 0.2$ at $N = 8, 16, 32$. It shows clearly that the behavior of $w_{\rm R}(x)$ depends much on the order of the two limits $\mu \to 0$, $N \to \infty$.

Let us next turn to $\rho_{\rm R}^{(0)}(x)$. In Fig. 4 we plot it for various N at $\mu = 0.2$. At small N the distribution is peaked near the origin and the dependence on N is small. At sufficiently large N the peak moves to $x \sim \mu$ and starts to grow, which is consistent with the large N result $\langle\nu_{\rm R}\rangle_0 = \mu$. Empirically

we find that the transition occurs at

$$N_{\rm c} = \frac{0.25 \sim 0.3}{\mu^2} \ . \tag{6.3}$$

Thus the distribution $\rho_{\rm R}^{(0)}(x)$ for the phase-quenched model also depends much on the order of the two limits $\mu \to 0$, $N \to \infty$. This can be seen more clearly in Fig. 5, where we plot the VEV $\langle \nu_{\rm R} \rangle_0$ against μ for various N. In particular the derivative $\frac{\partial}{\partial \mu} \langle \nu_{\rm R} \rangle_0$ becomes 0 if one takes the $\mu \to 0$ limit first, but it becomes 1 if one takes the $N \to \infty$ limit first.

The product $\rho_{\rm R}^{(0)}(x)\, w_{\rm R}(x)$ gives the unnormalized distribution for $\nu_{\rm R}$ in the full model, which we plot in Fig. 6. The distribution itself, even after appropriate normalization, has the noncommutativity, but the VEV $\langle \nu_{\rm R} \rangle$ calculated by the formula (5.9) is always closed to zero (see Table 1). The reason depends on the order of the two limits. If we take the $N \to \infty$ limit first, the positive and negative regions of $\rho_{\rm R}(x)$ cancel each other in the calculation of the first moment. If we consider small μ first, the distribution is peaked around the origin, which makes the first moment close to zero. Thus the noncommutativity cancels in the end result for the VEV $\langle \nu_{\rm R} \rangle$.

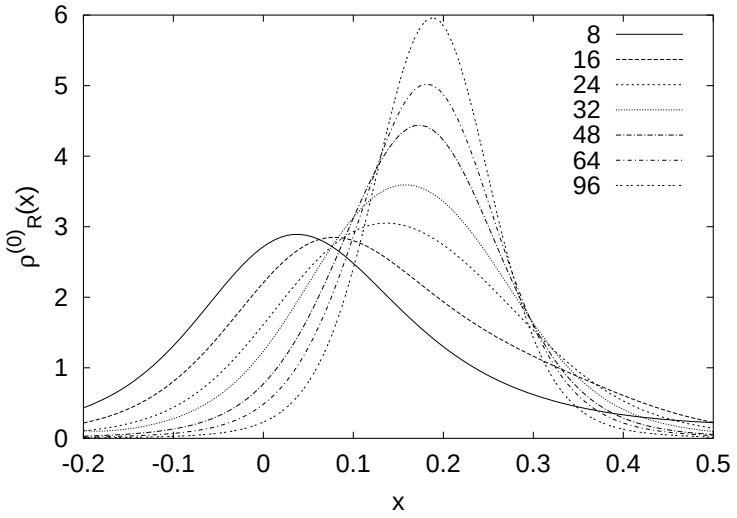

Figure 4. The function $\rho_{\rm R}^{(0)}(x)$ is plotted for $\mu = 0.2$ at various N.

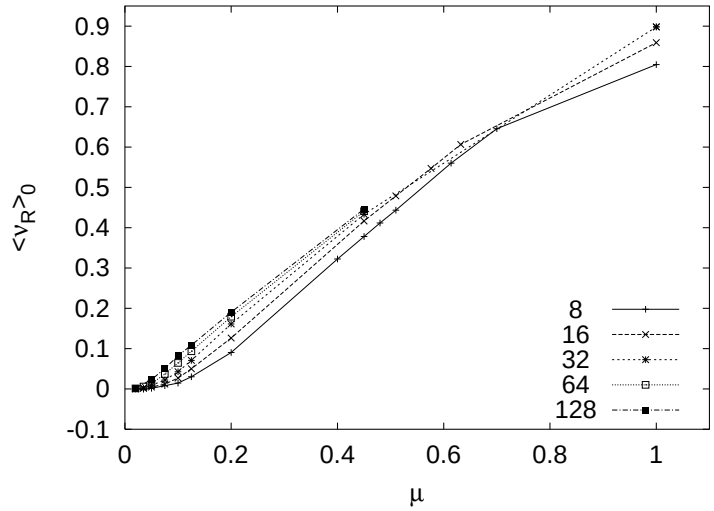

Figure 5. The VEV $\langle \nu_{\rm R} \rangle_0$ is plotted against μ for various N.

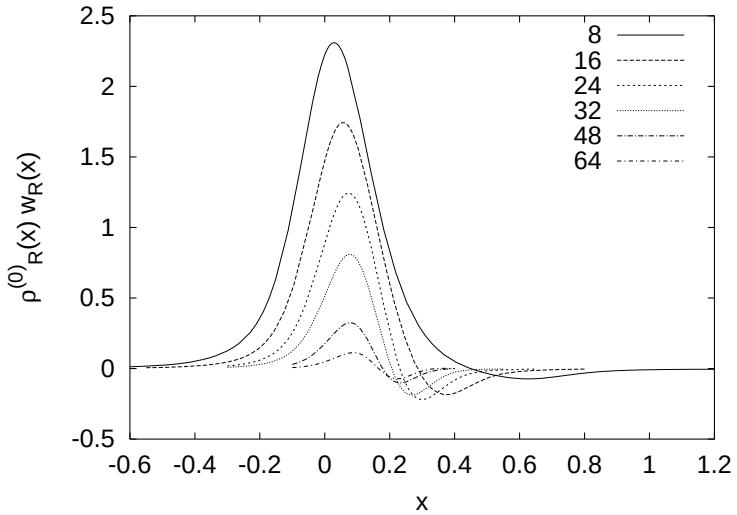

Figure 6. The product $\rho_{\rm R}^{(0)}(x) w_{\rm R}(x)$, which gives the unnormalized distribution for $\nu_{\rm R}$ in the full model, is plotted for $\mu = 0.2$ at various N.

7. Concluding remarks

The factorization method has been applied also to other systems with complex actions. In the original paper [12], it was used to study the dynamical generation of space time in superstring theory based on its matrix model formulation [17]. In this case the weight factors turned out to be positive definite, which enabled us to use their scaling property to make an extrapolation to larger system size. The method [18] proposed for simulating θ-vacuum like systems can be regarded as a special case of the factorization method. Promising results are obtained in the 2d CP^3 model etc.

Acknowledgments

This work is partially supported by Grant-in-Aid for Scientific Research (No. 14740163) from the Ministry of Education, Culture, Sports, Science and Technology.

References

1. D. Bailin and A. Love, *Phys. Rept.* **107**, 325 (1984).
2. D. T. Son, *Phys. Rev.* **D59**, 094019 (1999).
3. T. Schafer and F. Wilczek, *Phys. Rev.* **D60**, 114033 (1999).
4. M. G. Alford, K. Rajagopal and F. Wilczek, *Phys. Lett.* **B422**, 247 (1998).
5. R. Rapp, T. Schafer, E. V. Shuryak and M. Velkovsky, *Phys. Rev. Lett.* **81**, 53 (1998).
6. J. B. Kogut, D. Toublan and D. K. Sinclair, *Nucl. Phys.* **B642**, 181 (2002).
7. J. B. Kogut and D. K. Sinclair, *Phys. Rev.* **D66**, 034505 (2002).
8. Z. Fodor and S. D. Katz, *J. High Energy Phys.* **03**, 014 (2002).
9. C. R. Allton *et al.*, *Phys. Rev.* **D66**, 074507 (2002).
10. P. de Forcrand and O. Philipsen, *Nucl. Phys.* **B642**, 290 (2002).
11. M. D'Elia and M. P. Lombardo, *Phys. Rev.* **D67**, 014505 (2003).
12. K. N. Anagnostopoulos and J. Nishimura, *Phys. Rev.* **D66**, 106008 (2002).
13. J. Ambjørn, K. N. Anagnostopoulos, J. Nishimura and J. J. Verbaarschot, *J. High Energy Phys.* **10**, 062 (2002).
14. M. A. Stephanov, *Phys. Rev. Lett.* **76**, 4472 (1996).
15. J. Ambjørn, K. N. Anagnostopoulos, J. Nishimura and J. J. Verbaarschot, in preparation.
16. M. A. Halasz, A. D. Jackson and J. J. Verbaarschot, *Phys. Rev.* **D56**, 5140 (1997).
17. N. Ishibashi, H. Kawai, Y. Kitazawa and A. Tsuchiya, *Nucl. Phys.* **B498**, 467 (1997) .
18. V. Azcoiti, G. Di Carlo, A. Galante and V. Laliena, *Phys. Rev. Lett.* **89**, 141601 (2002).